Automated Quantification of Adipose Tissue Distribution in Children Using a 2-point Dixon Technique

J. Kullberg[1], P-A. Svensson[2], A-K. Karlsson[3,4], E. Stokland[2], and J. Dahlgren[3,4]
[1]Department of Radiology, Uppsala University, Uppsala, Sweden, [2]Department of Pediatric Radiology, The Sahlgrenska University Hospital, Göteborg, Sweden, [3]Institute of Clinical Sciences, Sahlgrenska Academy, University of Gothenburg, Göteborg, Sweden, [4]The Queen Silvia Children's Hospital, Göteborg, Sweden

Introduction: The high prevalence of overweight and obesity is a large health problem in many parts of the world [1]. Many children establish overweight or obesity in early childhood and these individuals risk remaining in that condition throughout life [2]. Both the total amounts of adipose tissue (AT), as well as its distribution, are well known health risk factors [3]. MRI allows assessment of both amount and distribution of AT. Automated segmentation algorithms have the potential to remove the bias introduced by manual assessments. Most of the automated methods developed and validated have focused on assessments in adult subjects. Measurements in children add two main challenges. The first is the compliance to the MR procedure. Generally, the younger the child is, the more challenging is the MR imaging. Secondly, children are smaller and have less AT, which reduces relative assessment accuracy.

Methods: The subjects included in this study were 21 healthy children (10 girls, 11 boys) of age 5 (BMI 14.8±1.2kg/m^2). Imaging was performed with a 1.5T clinical MR system (Signa HDx Twinspeed, GE Medical Systems, WI, USA). A T1-weighted 3D dual gradient-echo sequence (LAVA-FLEX, supplied by GE Medical Systems) that acquired fat/water images in one acquisition using an 8-channel cardiac coil and a 2-point Dixon technique was used. A volume of 16 transversal 10 mm thick slices was centred over L4. Scan parameters were: TR 6.5ms, TEs 2.4, 4.8ms, flip angle 12 deg, FOV 32x24 cm, matrix 256x128, NEX 0.7. Reconstructed voxel size 1.25x1.25x10mm. Imaging time 6 s.
The fully automated analysis used the water and fat images to measure the volumes of visceral and subcutaneous AT (VAT and SAT). The main steps of the algorithm are illustrated in Fig 1. Firstly, the water and fat images are used to calculate three other basic images denoted sum (water + fat), fat fraction (fat/sum), and water fraction (water/sum) respectively, see Fig 1a-e. The abdomen was separated from background and arms by use of fuzzy clustering (Liew2003) of the water, fat and sum images into three classes (AT, muscle/organs, and background) in combination with morphological operations. The background cluster is shown in Fig 1f. A weak "belongingness" (<10%) to the background cluster was used as the binary classification of the body. AT was determined from the fat fraction image by thresholding at 50% fat content, Fig 1g. A binary mask (mask1) was used to separate the SAT from the rest of the abdomen, Fig 1h. Mask1 was created by thresholding the water fraction image at 50% water content. All but the largest connected object in 3D was then removed to reduce the response from water-signal in the SAT and skin regions. A slice-wise convex hull was then used to ensure that the mask1 was a closed convex object. The SAT was determined as the AT "outside" mask1. Since mask1 was convex SAT might be excluded in non-convex regions of the abdominal muscles. To correct for this, the SAT region was allowed to extend inwards (for an empirically determined distance) by including connected AT-pixels. The VAT was determined as the AT inside the mask1 after exclusion of bone marrow (BM) and intramuscular AT (IMAT). The exclusion was performed by use of a geometrical pelvis probability model, Fig 1i. The model was created by summing distance transforms of manual delineations in eight subjects, not included in this study, of the same age. VAT and SAT reference segmentations were created to evaluate the automated segmentations of VAT and SAT. The reference measurements were created by semi-automated segmentation of the calculated fat fraction images. Three operators manually delineated the VAT region and the regions containing BM and IMAT in all slices. The VAT reference was determined by the voxels with fat fraction greater than 50% inside the manually delineated VAT region. The SAT reference was determined as the voxels, inside the body masks, outside the manually delineated regions of VAT, BM, and IMAT, with fat fraction greater than 50%. For objective suppression of random fat fractions from low MR signal regions the same suppression as in the automated approach was used.

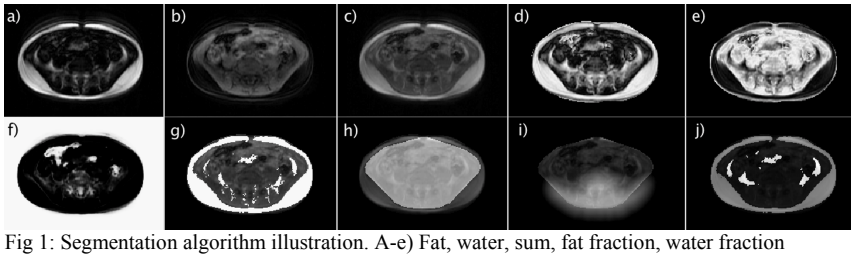

Fig 1: Segmentation algorithm illustration. A-e) Fat, water, sum, fat fraction, water fraction images. F) Background cluster, g) thresholded adipose tissue, h) mask1, i) pelvis probability model, j) segmented VAT and SAT.

Results: The correlations between the mean reference and the automatically segmented volumes were 0.977 and 0.999 for VAT and SAT, respectively. The VAT volumes from the automated segmentation were not seen to differ from the manually segmented (Auto - Manual = -4.0%±10.3%). However, the automatically segmented SAT volumes were underestimated by 9.4%±3.8% compared to the manually segmented volumes. The precision results for the automatically determined volumes of VAT and SAT are shown in Fig 2. For VAT, True positive (TP) and False Positive (FP) values were 87%±9% and 14%±9%, respectively. For SAT, the values were 90%±3% and 0.0%±0.0%, respectively. The automated segmentation required, on average, 31 seconds per abdomen, when executed on an Intel 2.40GHz, 2GB PC, while the manual segmentation required on average 16.9 minutes.

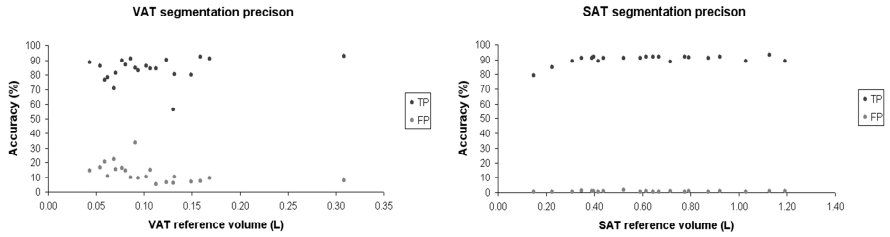

Fig 2: Accuracy (True Positive, TP and False Positive, FP) of the automated VAT and SAT segmentations.

Conclusion: We have presented and validated an imaging protocol which, in combination with a fully automated post processing, allows time efficient and robust analysis of body composition in young children.

References: [1] Dietz WH. *BMJ* 2001;322(7282):313-314. [2] He Q, Karlberg J. *Pediatr Res* 1999;46(6):697-703. [3] Weiss R, Dufour S, Taksali SE, et al. *Lancet* 2003;362(9388):951-957. [4] Liew AW, Yan H. *IEEE Trans Med Imaging* 2003;22(9):1063-1075.